Downregulation of histone-lysine N-methyltransferase EZH2 inhibits cell viability and enhances chemosensitivity in lung cancer cells

ZIYANG CAO*, WEI WU*, HAITING WEI, WEI ZHANG, YAN HUANG and ZHENGWEI DONG

Department of Pathology, Shanghai Pulmonary Hospital, School of Medicine, Tongji University, Shanghai 200433, P.R. China

Received December 16, 2019; Accepted May 13, 2020

DOI: 10.3892/ol.2020.12287

Abstract. Histone-lysine N-methyltransferase EZH2 (EZH2) is the principle component of the polycomb repressive complex 2 (PRC2)/embryonic ectoderm development protein-EZH2 complex, which promotes tumorigenesis by repressing transcription of tumor suppressor genes. EZH2 is considered a key marker in several types of cancer, such as colorectal and prostate cancer. However, the molecular mechanisms and clinical value of EZH2 in lung cancer have not yet been fully investigated. The aim of the present study was to investigate the functions of EZH2 in lung cancer progression and to determine whether treatment with an EZH2 inhibitor enhanced the chemosensitivity of lung cancer cells to cisplatin (CDDP). At the logarithmic growth phase, A549 cells were treated with a small interfering (si)RNA-EZH2, and cell viability was detected using an MTT assay. The degree of apoptosis and cell cycle were detected using flow cytometry. Cell migration and invasion were detected via wound healing and Transwell Matrigel assays. According to information from the Gene Expression Omnibus database, the results of the present study demonstrated that EZH2 was upregulated in lung cancer. Furthermore, overexpression of EZH2 was associated with poor patient prognosis, while EZH2 knockdown inhibited cell viability and migration, and enhanced apoptosis and chemosensitivity in a lung cancer cell line. EZH2 knockdown and treatment of A549 cells using EZH2 inhibitor elevated the inhibitory effects of CDDP on cell viability and apoptosis. Western blot and reverse transcription-quantitative PCR analyses were performed to assess the expression levels of relative protein and mRNA, respectively, in A549 cells treated with siRNA-EZH2 or with CDDP. Overall, the results of the present study demonstrated that high EZH2 expression was associated with poor prognosis, accompanied with a potential impairment of migration and viability in lung cancer cells. These findings suggest that EZH2 may act as a candidate molecular target for gene therapy, and treatment with EZH2 inhibitor may be used to increase chemosensitivity to CDDP agents in lung cancer.

Correspondence to: Dr Yan Huang or Dr Zhengwei Dong, Department of Pathology, Shanghai Pulmonary Hospital, School of Medicine, Tongji University, 507 Zhengmin Road, Shanghai 200433, P.R. China
E-mail: huangyan10180826@sina.com
E-mail: zhengweidong@genopub.com

*Contributed equally

Key words: histone-lysine N-methyltransferase EZH2, lung cancer, apoptosis, chemosensitivity

Introduction

Lung cancer is one of the most common primary malignant tumors. According to the 2018 Global Cancer Statistics, lung cancer was the leading cause of cancer-associated mortality worldwide, with a 5-year survival rate of patients with lung cancer of 18% (1). The most common causes of lung cancer include smoking, air pollution, heredity factors and activation of cancer genes, such as Ras and Raf (2). Despite the fact that the majority of patients at early disease stages can be treated with surgery (3), the choice of treatment for patients at advanced stages are limited to radiotherapy and chemotherapy (4). Furthermore, in some patients, prolonged exposure to a single chemotherapeutic agent such as cisplatin may lead to the development of resistance (5). Thus, the development of novel targeted therapeutic strategies remains critical for improved prognosis and survival outcomes of patients with lung cancer.

Histone-lysine N-methyltransferase EZH2 (EZH2) is the core catalytic component of polycomb repressive complex 2 (PRC2), which is involved in transcriptional repression (6). EZH2 is considered an oncogene, as it is frequently overexpressed in several types of human cancer, including prostate (7), gastric (8) and breast cancer (9,10). Furthermore, RNA interference of EZH2 has been reported to significantly decrease cell viability in breast cancer (11,12). However, the molecular mechanisms by which EZH2 knockdown inhibits disease progression of lung cancer remain unclear.

The aim of the present study was to identify whether EZH2 was associated with cell viability, migration and invasion, as

well as cell cycle progression and apoptosis, in the lung cancer A549 cell line. By identifying whether EZH2 acts as an oncogene in lung cancer, the present study may provide a novel diagnostic biomarker and a therapeutic target for the treatment of lung cancer.

Materials and methods

Bioinformatics analysis of human lung cancer. The GSE19804 dataset (13) was downloaded from the Gene Expression Omnibus (GEO) database (https://www.ncbi.nlm.nih.gov/geo) using the keywords 'lung cancer', 'Homo sapiens' and 'Expression profiling by array or sequencing', which includes 60 adjacent non-tumor (within 2 cm around tumors) and 60 tumor samples. GEO2R is an interactive online platform, which identifies differentially expressed genes (DEGs) by comparing samples in the GEO series (14). The cut-off criteria for the DEGs were an adjusted $P<0.05$ and a $|\log_2$ fold change (FC)$|$ value of >2. The genes were aligned using their expression levels, and the data are presented as a volcano plot and a heat map. PROGgeneV2 (http://watson.compbio.iupui.edu/chirayu/proggene/database/?url=progge) is a web-based platform used to study prognostic implications of genes in different types of cancer. PROGgeneV2 was used to perform the survival analysis based on EZH2 expression in the GSE30219 dataset (15) downloaded from the GEO database.

Materials and reagents. The cell cycle kit (cat. no. 558662) and apoptosis detection kit (cat. no. 559763) were purchased from BD Biosciences, while the MTT reagent was purchased from Sigma-Aldrich; Merck KGaA. The primary antibodies (all diluted 1:1,000) against EZH2 (cat. no. 4905), cyclin D1 (cat. no. 2922), p21 (cat. no. 2947), cleaved(C)-caspase-3 (cat. no. 9661), C-caspase-9 (cat. no. 52873), N-cadherin (cat. no. 4061), E-cadherin (cat. no. 3195), vimentin (cat. no. 5741) and GAPDH (cat. no. 5174) were purchased from Cell Signaling Technology, Inc., and the EZH2 inhibitor (EPZ-6438) was obtained from Selleck Chemicals.

Cell culture. A total of five human lung cancer cell lines (H1650, PC9, A549, H1299 and H460), and a normal lung epithelium cell line, (BEAS-2B) were purchased from the Bank of Type Culture Collection of the Chinese Academy of Sciences and cultured in RPMI-1640 medium supplemented with 10% FBS and 100 U/ml penicillin (Gibco; Thermo Fisher Scientific, Inc.) at 37˚C in a humidified incubator with 5% CO_2.

Reverse transcription-quantitative (RT-q)PCR. Total RNA was extracted from lung cancer A549 cells using TRIzol® regent (Invitrogen; Thermo Fisher Scientific, Inc.) according to the manufacturer's protocol, and cDNA was generated using the PrimeScript™ RT reagent kit (Takara Biotechnology Co., Ltd.) at 37˚C for 30 min, according to the manufacturer's protocol. qPCR was subsequently performed using SYBR® Premix ExTaq™ (Takara Biotechnology Co., Ltd.) according to the manufacturer's protocol and detected using the LightCycler™ 480 system (Roche Diagnostics). The reaction conditions were as follows: Initial denaturation at 95˚C for 3 min, followed by 40 cycles of denaturation at 95˚C for 10 sec, annealing at 60˚C for 40 sec and extension at 72˚C for 40 sec. The following primer sequences were used for qPCR: EZH2 forward, 5'-GAAAGCCGCCCACCTC-3' and reverse, 5'-AAACATCGCCTACAGAAAAGC-3'; and GAPDH forward, 5'-GGAGCGAGATCCCTCCAAAAT-3' and reverse, 5'-GGCTGTTGTCATACTTCTCATGG-3'. Relative expression levels were calculated using the $2^{-\Delta\Delta Cq}$ method and normalized to the internal reference gene GAPDH (16).

Western blot analysis. Total protein was extracted from A549 cells using RIPA lysis buffer supplemented with protease inhibitors cocktail and PMSF (1:100) (all Beyotime Institute of Biotechnology). Protein concentration was determined using the Pierce Micro BCA protein assay system (Pierce; Thermo Fisher Scientific, Inc.). A total of 50 μg protein/lane was separated using SDS-PAGE on a 10% gel and subsequently transferred onto polyvinylidene difluoride membranes (Sigma-Aldrich; Merck KGaA). The membranes were blocked with 5% skimmed milk in TBS-Tween (1% Tween-20) for 1 h at room temperature. After washing with TBS-Tween, the membranes were incubated with primary antibodies against EZH2, cyclin D1, p21, C-caspase-3, C-caspase-9, N-cadherin, E-cadherin, vimentin and GAPDH overnight at 4˚C. After washing, membranes were incubated with goat anti-rabbit secondary antibody (1:2,000; cat. no. 7074; Cell Signaling Technology, Inc.) at room temperature for 1 h. Protein bands were visualized using an enhanced chemiluminescence kit (cat. no. NCI4106; Thermo Fisher Scientific, Inc.) and scanned using the lmageQuant 4000 system (Cytiva). The optical density of the target bands were quantified using the Quantity One system v4.6.2 (Bio-Rad Laboratories, Inc.).

RNA interference. A549 cells were transfected with 50 nM EZH2 small interfering (si)RNA (Shanghai Genechem Co., Ltd.) using Lipofectamine® 3000 reagent (Invitrogen; Thermo Fisher Scientific, Inc.) for 48 h before subsequent experimentation, according to the manufacturer's protocol. The following siRNA sequences were used: EZH2 forward, 5'-GTGCCCTTGTGTGATAGCACAA-3' and reverse, 5'-GGCACTTTCATTGAAGAACTAA-3'; and non-targeted negative control (NC) forward, 5'-UUCUCCGAACGUGUCACGUTT-3' and reverse, 5'-ACGUGACACGUUCGGAGAATT-3'.

MTT assay. The viability of cells was detected using the MTT assay, according to the manufacturer's protocol. Briefly, A549 cells were trypsinized and seeded into 96-well plates at a density of $1x10^4$, following siRNA transfection for 48 h or treatment with EPZ-6438 (40 μM) for 24 h, and treatment with different concentrations (0, 2, 4, 8 or 16 μM) of cisplatin (CDDP; Sigma-Aldrich; Merck KGaA) for 24 h. Cells were subsequently incubated with 20 μl MTT solution (in 5 mg/ml PBS) at 37˚C for 4 h. Following which, the purple formazan crystals were dissolved using 150 μl dimethyl sulfoxide for 20 min at room temperature, and cell viability was subsequently analyzed at a wavelength of 570 nm. All experiments were performed in triplicate.

Colony formation assay. A total of 500 A549 cells were plated into 35 mm dishes prior to transfection with siRNA or treatment with EPZ-6438 (40 μM) for 24 h, followed by treatment with 4 μM CDDP for 24 h, and maintained at 37˚C for 2 weeks.

Cell colonies were subsequently washed three times with PBS, fixed with ethanol for 15 min at room temperature and stained with 1% crystal violet for 20 min at room temperature. Cell colonies were observed using a Canon camera (Canon, Inc.).

Cell cycle assay. Cell cycle analysis was performed using propidium iodide (PI) staining (BD Biosciences), according to the manufacturer's protocol. Briefly, cells were digested with EDTA-free trypsin and centrifuged at 500 x g for 5 min at 4˚C. A total of $1x10^6$ cells were harvested and fixed with 70% ethanol overnight at 4˚C. Subsequently, PI supplemented with RNase A was added and the DNA content was sorted using flow cytometric analysis (BD Biosciences). Total cell quantity at each phase was analyzed using ModFit LT v5.0 software (Verity Software House, Inc.).

Flow cytometric analysis of apoptosis. The extent of apoptosis was determined using the PE-Annexin V Apoptosis assay kit (BD Biosciences), according to the manufacturer's protocol. Briefly, cells were digested with EDTA-free trypsin and centrifuged at 500 x g for 5 min at 4˚C. Cells were harvested and washed three times with PBS, 48 h post-transfection, prior to resuspension in 500 μl binding buffer. Subsequently, cells were incubated with 5 μl PI and 5 μl Annexin V-FITC in the dark at room temperature for 10 min and apoptotic cells were analyzed using the FACScan flow cytometer (BD Biosciences).

Wound healing assay. A total of $1x10^5$ cells/well were seeded into 24-well plates and cultured in RPMI-1640 supplemented with 1% penicillin, 1% streptomycin and 10% FBS at 37˚C in 5% CO_2 until they reached 90% confluence. Subsequently, the cell monolayers were scratched using a 200 μl pipette tip to produce a consistent width. Cells were washed twice with PBS to remove non-adherent cells, while the adherent cells were serum-starved in serum-free medium overnight. Migratory cells were observed in five randomly selected fields under a light microscope (magnification, x40) at 0 and 24 h. The width of the wounds was measured using ImageJ software 1.52 (National Institutes of Health).

Transwell and Matrigel assays. The migration and invasion assays were performed as previously described (17). Briefly, $4x10^4$ cells were plated in the upper chambers of 8-μM-pore sized Transwell plates (BD Biosciences) in serum-free medium and cultured for 37˚C for both assays. A Matrigel assay was performed to detect cell invasion. The Transwell membranes were precoated with 50 μl Matrigel (1 mg/ml; BD Biosciences) at 37˚C for 4 h. A total of 500 μl RPMI-1640 supplemented with 10% FBS was added to the lower chambers. Following incubation at 37˚C in 5% CO_2 for 24 h, both the migratory and invasive cells in the lower chambers were washed twice with PBS and fixed with ethanol for 10 min at room temperature. Non-invasive cells in the upper chambers were removed using a cotton swab. Invasive cells, and the migratory cells were stained with 1% crystal violet for 20 min at room temperature. Stained cells were observed under a light microscope (magnification, x100).

Statistical analysis. Statistical analysis was performed using GraphPad Prism software version 7.0 (GraphPad Software, Inc.). The survival curve was calculated using the Kaplan-Meier estimator method and the log-rank test was used to compare the two survival curves. Data are presented as the mean ± standard deviation of three independent experiments. Unpaired Student's t-test was used to compare differences between two groups, while one-way ANOVA followed by the least significant difference post hoc test was used to compare difference between multiple groups. $P<0.05$ was considered to indicate a statistically significant difference.

Results

EZH2 expression is upregulated in human lung cancer. Analysis of the GSE19804 dataset identified 265 DEGs, including 53 upregulated and 212 downregulated DEGs in lung cancer compared with normal tissues ($P<0.05$ and $|Log_2FC| >2$; Fig. 1A). The DEGs are shown in Table SI, while the top 20 DEGs in lung cancer are presented in Fig. 1B.

Survival analysis was performed for patients with lung cancer, using the GSE30219 dataset. The results demonstrated that high EZH2 expression was associated with a shorter overall survival time in patients with lung cancer, thus an unfavorable prognosis, compared with those with low EZH2 expression. The 3- and 5-year survival rates of patients with high EZH2 expression were lower than those of patients with low EZH2 expression (Fig. 1C).

EZH2 mRNA and protein expression levels were also determined in the six lung cancer cell lines using RT-qPCR and western blot analyses. The results show that EZH2 was upregulated in all the lung cancer cell lines (H1650, PC9, A549, H1299 and H460) compared with that in the BEAS-2B cell line (Fig. 1D). As the expression level of EZH2 was highest in the A549 cell line, this was used for further experimentations. Taken together, these results suggest that EZH2 may be associated with tumorigenesis and progression of lung cancer.

EZH2 knockdown restricts cell viability and induces apoptosis. To evaluate the function of EZH2 in lung cancer cells, A549 cells were transfected with siRNA-EZH2, and non-targeting siRNA was used as the NC. The results demonstrated that the mRNA and protein expression levels of EZH2 were significantly decreased in A549 cells transfected with siRNA-EZH2 compared with that in the NC cells, using RT-qPCR and western blot analyses, respectively (Fig. 2A).

To determine the biological function of EZH2 in lung cancer cells, the viability of A549 cells following EZH2 knockdown was analyzed using MTT and colony-formation assays. The MTT assay results demonstrated that the cell viability was significantly decreased in siRNA-EZH2 transfected cells compared with that in the NC cells (Fig. 2B). Similarly, colony formation ability was also decreased following EZH2 knockdown (Fig. 2C). In addition, EZH2 knockdown also induced G_1 phase cell cycle arrest, while the cell percentage in the G_2 phase was also decreased in A549 cells (Fig. 2D).

Flow cytometric analysis was performed to determine whether the inhibitory effects on cell viability were associated with apoptosis, following EZH2 knockdown (Fig. 2E). The number of cells in early stage apoptosis was significantly higher in the cells treated with EZH2 siRNA compared with that in the NC cells, 0.7±0.21 vs. 2.9±0.48% cells ($P<0.05$).

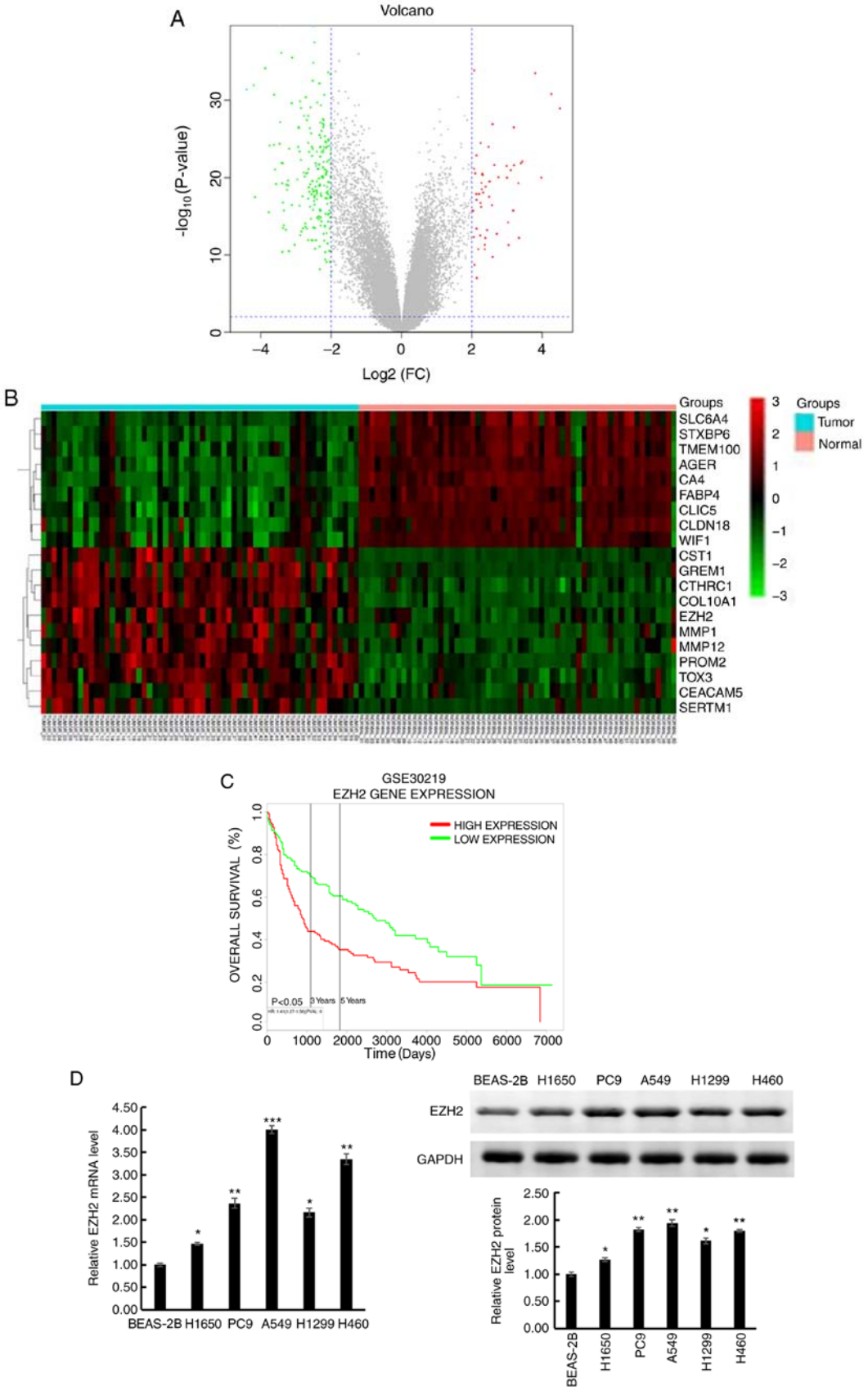

Figure 1. EZH2 expression is upregulated in human lung cancer tissues and cell lines. (A) Differentially expressed genes were selected using volcano plot filtering (P<0.05; FC >2). The red dots represent upregulated genes, while the green dots represent downregulated genes and the grey dots represent genes with |FC|<2. (B) Heatmap of the top 20 dysregulated genes. Red indicates upregulation and green indicates downregulation. The values between -3 and 3 indicate the FC degree in gene expression. The 60 GSM on the left side were collected from tumor tissues of patients with lung cancer, while the 60 GSM on the right side were collected from normal tissues of the same patients. (C) Altered EZH2 expression was demonstrated to be associated with overall survival time. (D) EZH2 expression in lung cancer cell lines (H1650, PC9, A549, H1299 and H460) and normal human lung epithelial cell line (BEAS-2B) was detected using reverse transcription-quantitative PCR and western blot analyses. Data are presented as the mean ± standard deviation of three independent experiments. *P<0.05, **P<0.01, ***P<0.001 vs. BEAS-2B. EZH2, histone-lysine N-methyltransferase EZH2; FC, fold change; GSM, Gene Expression Omnibus samples.

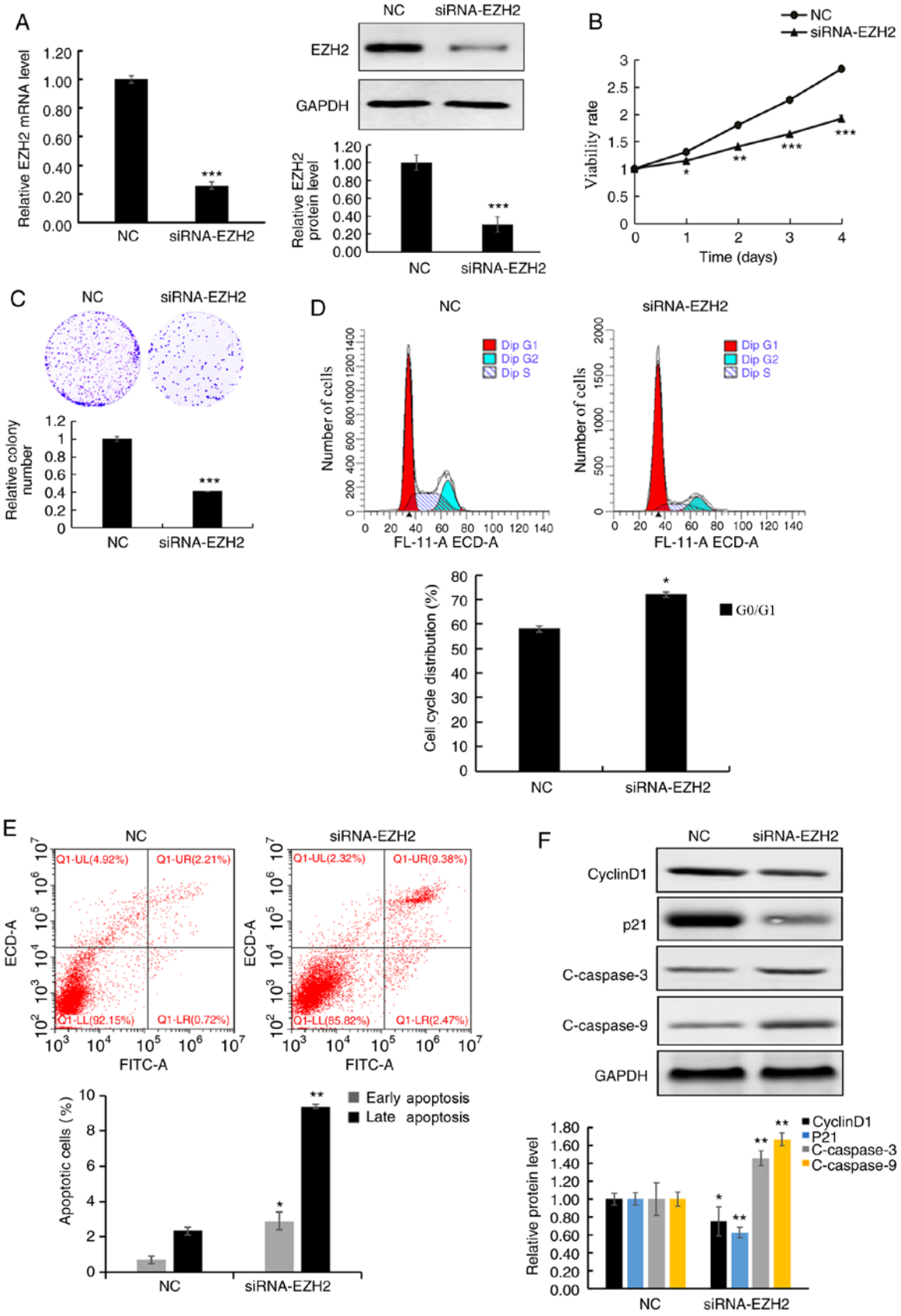

Figure 2. EZH2 knockdown inhibits cell viability and induces apoptosis. (A) EZH2 mRNA and protein expression levels were significantly decreased in cells transfected with siRNA-EZH2 compared with that in the NC. (B) MTT assay demonstrated that the viability of A549 cells deceased following EZH2 knockdown. (C) The colony formation assay was performed using A549 cells, with or without EZH2 knockdown. (D) The cell cycle distribution was analyzed using flow cytometry, with or without EZH2 knockdown and analyzed quantitatively. (E) NC and siRNA-EZH2 transfected cells were stained with Annexin V/propidium iodide for flow cytometric analysis and analyzed quantitatively. (F) Western blot analysis of cyclin D1, p21, C-caspase-3 and -9 proteins in A549 cells, treated with NC and siRNA-EZH2 and analyzed quantitatively. Data are presented as the mean ± standard deviation of three independent experiments. *P<0.05, **P<0.01 and ***P<0.001 vs. NC. EZH2, histone-lysine N-methyltransferase EZH2; si, small interfering; NC, negative control; C, cleaved; FITC, fluorescein isothiocyanate.

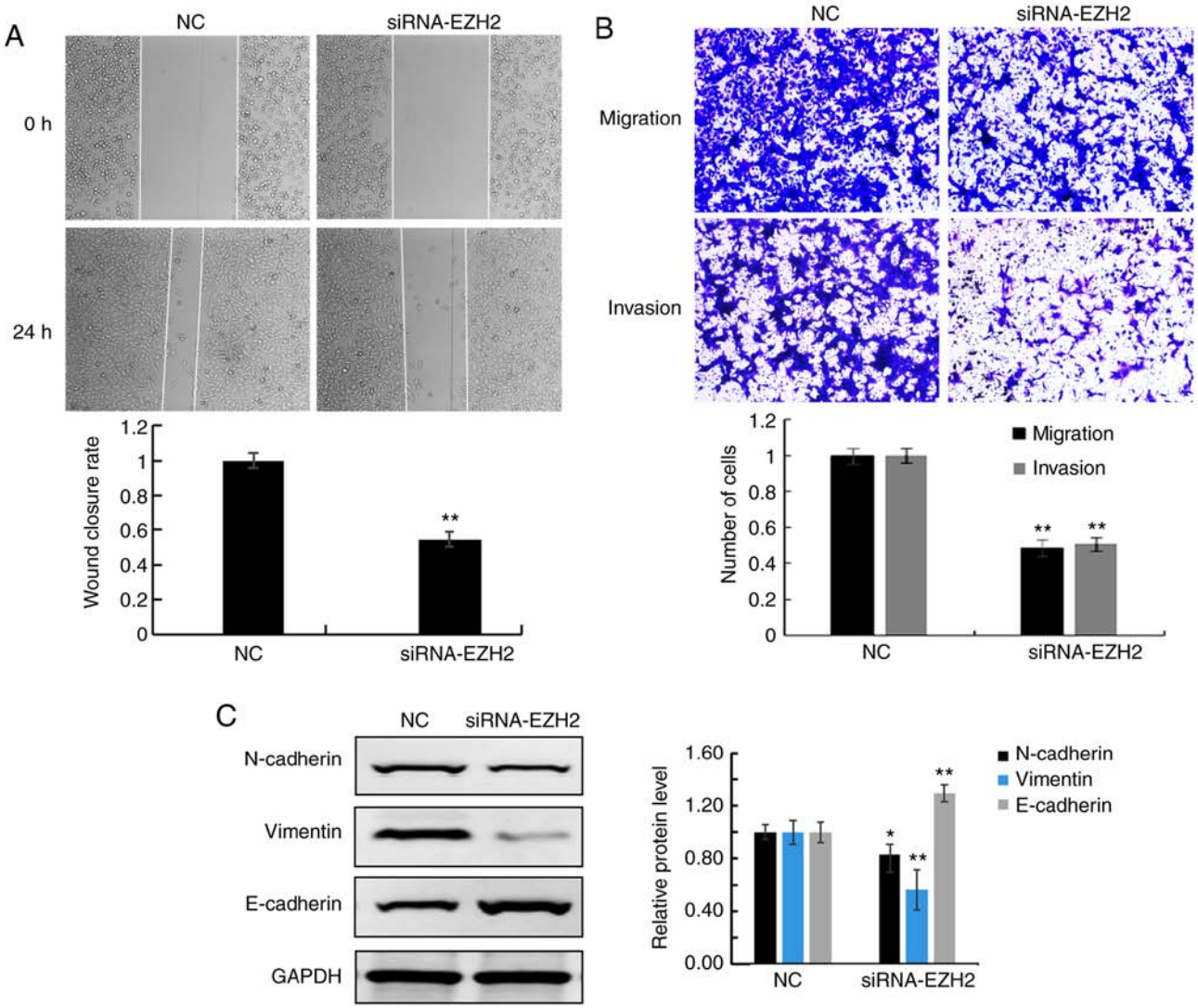

Figure 3. EZH2 knockdown inhibits cell migration and invasion in lung cancer cells. (A) Wound healing and (B) Transwell and Matrigel assays were used to detect the migration and invasion of lung cancer cells treated with NC and siRNA-EZH2 and analyzed quantitatively. Magnification, x40. (C) The protein expression levels of N-cadherin, E-cadherin and vimentin were detected in cells transfected with NC and siRNA-EZH2 and analyzed quantitatively. Data are presented as the mean ± standard deviation of three independent experiments. *P<0.05 and **P<0.01 vs. NC. EZH2, histone-lysine N-methyltransferase EZH2; NC, negative control; si, small interfering.

In addition, the percentage of apoptotic cells in late stage apoptosis was also significantly increased in siRNA-EZH2 transfected cells compared with that in the NC cells. Furthermore, the protein expression levels of the cell cycle proteins, cyclin D1 and p21 significantly decreased, while the levels of the apoptosis-associated proteins, C-caspase-3 and -9 significantly increased in cells following EZH2 knockdown (Fig. 2F). These results indicate that EZH2 may play a role in regulating cell viability and apoptosis.

EZH2 knockdown inhibits cell migration and invasion. The migratory ability of A549 cells was assessed using wound healing and Transwell assays. Both assays revealed that the migratory rate was decreased in A549 cells transfected with EZH2 siRNA compared with that in the NC cells (Fig. 3A and B, respectively). In addition, the Matrigel assay found that A549 invasion was also decreased in cells transfected with EZH2 siRNA compared with that in the NC cells (Fig. 3B). Furthermore, decreased protein expression levels of epithelial-mesenchymal transition (EMT)-associated proteins (N-cadherin and vimentin), and increased levels of E-cadherin were detected in siRNA-EZH2 transfected cells compared with that in NC cells (Fig. 3C).

EZH2 knockdown enhances sensitivity of lung cancer cells to CDDP by inhibiting viability and enhancing apoptosis. To further assess the function of EZH2 during treatment with CDDP, the cell viability of NC and siRNA-EZH2 transfected cells following CDDP treatment was analyzed using the MTT and colony formation assays. The viability (Fig. 4A) and colony formation ability (Fig. 4B) of A549 cells transfected with siRNA-EZH2 were significantly reduced compared with that in NC cells, following CDDP treatment (0, 2, 4, 8 or 16 μM) and 4 μM CDDP treatment, respectively. To determine whether the chemo response effects of EZH2 on A549 cells was associated with apoptosis, transfected cells following CDDP treatment were detected using flow cytometry. The number of early stage apoptotic cells in the EZH2 knockdown

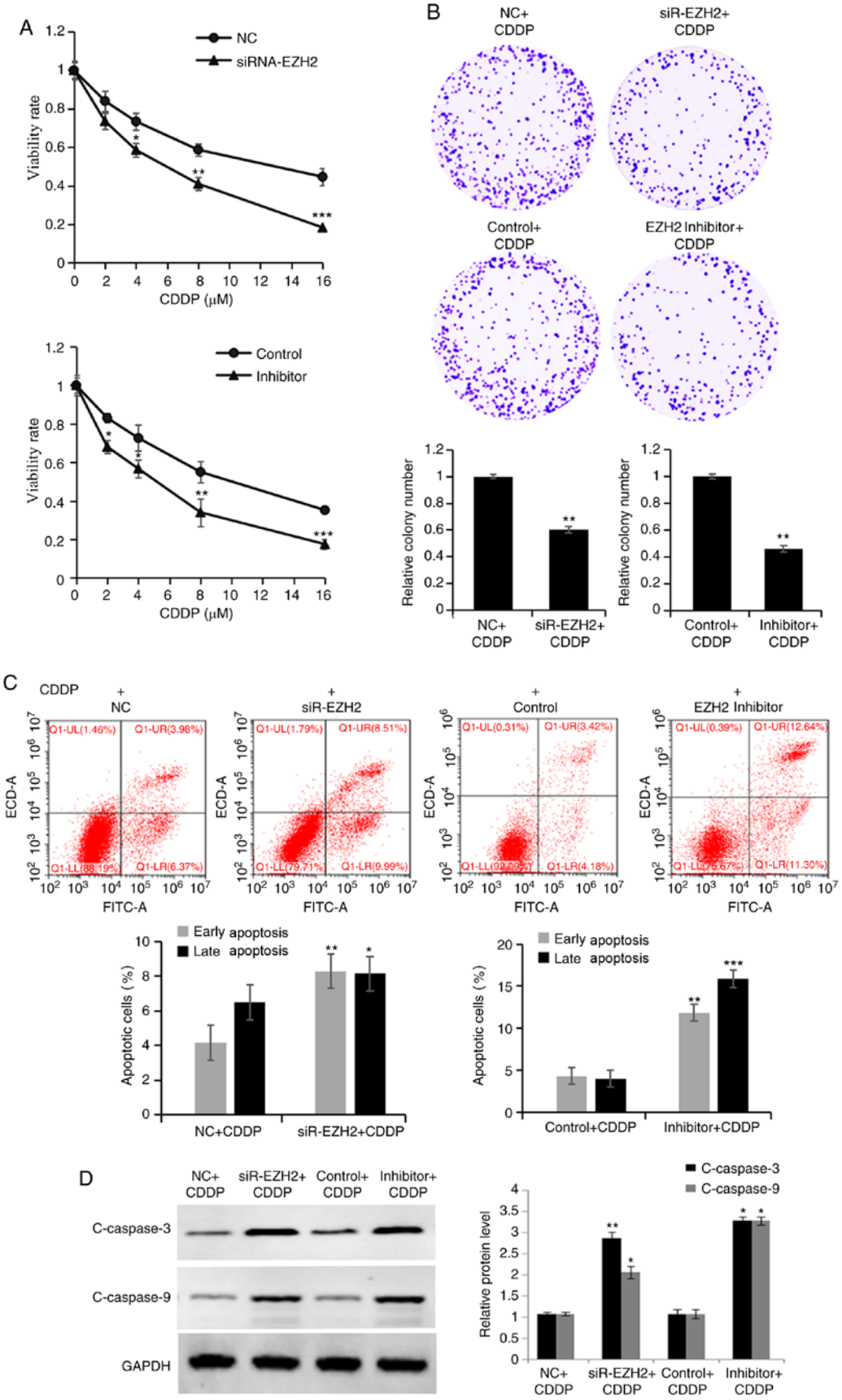

Figure 4. Downregulation of EZH2 enhances sensitivity to CDDP by inhibiting cell viability and promoting apoptosis. (A) MTT and (B) colony formation assays were performed to detect the proliferative ability of cells transfected with siRNA-EZH2 or treated with the EZH2 inhibitor, following CDDP treatment, respectively. (C) A higher apoptosis rate was observed in cells transfected with siRNA-EZH2 or treated with the EZH2 inhibitor, following CDDP treatment, compared with that in the control groups. (D) The expression levels of C-caspase-3 and -9 were detected using western blot analysis in cells transfected with siRNA-EZH2 or treated with the EZH2 inhibitor, following CDDP treatment. Data are presented as the mean ± standard deviation of three independent experiments. *P<0.05, **P<0.01 and ***P<0.001 vs. NC+CDDP or Control+CDDP. EZH2, histone-lysine N-methyltransferase EZH2; si, small interfering; NC, negative control; CDDP, cisplatin.

cells (9.99±1.26%) was significantly increased compared with that in the NC cells (6.37±0.69%), with 4 μM CDDP for 24 h (Fig. 4C). In addition, the percentage of late-stage apoptotic cells was significantly increased in EZH2 knockdown cells (8.51±0.94%) compared with that in the NC cells (3.98±0.43%), with 4 μM CDDP for 24 h. Furthermore, the expression levels of the apoptosis-associated proteins, C-caspase-3 and -9, increased in siRNA-EZH2 cells treated with CDDP compared with those in NC cells (Fig. 4D).

Notably, an inhibitor of EZH2 (EPZ-6438) was used to simulate EZH2 silencing. A549 cells treated with CDDP (4 μM) alone or in combination with EPZ-6438 (40 μM) for 24 h were subsequently analyzed using the MTT, colony formation and apoptosis assays. The viability (Fig. 4A) and colony formation ability (Fig. 4B) of A549 cells treated with the EZH2 inhibitor were significantly decreased compared with those in control cells, following CDDP treatment (0, 2, 4, 8 or 16 μM) and 4 μM CDDP treatment, respectively. The number of early stage apoptotic cells in cells treated with the EZH2 inhibitor (11.30±1.35%) was significantly increased compared with that in the control cells (4.18±0.53%); additionally, the percentage of late-stage apoptotic cells was significantly increased in cells treated with the EZH2 inhibitor (12.64±1.64%) compared with that in the control cells (3.42±0.31%), with 4 μM CDDP for 24 h (Fig. 4C). Furthermore, the expression levels of the apoptosis-associated proteins, C-caspase-3 and -9, increased in cells treated with the EZH2 inhibitor and with CDDP compared with those in control cells (Fig. 4D). Therefore, the results were consistent to those observed with siRNA-EZH2. Overall, the results of the present study demonstrated that EZH2 played a vital role in CDDP response, and EZH2 inactivation increased chemosensitivity to chemotherapeutic agents of lung cancer cells. Thus, EZH2 inhibitor may be used to be enhance chemosensitivity of lung cancer cells.

Discussion

According to the 2018 Global Cancer Statistics Report, lung cancer is the world's leading malignant tumor in morbidity (11.6%) and mortality (18.4%) rates (18). Both surgical resection or chemotherapy have become less effective in the treatment of lung cancer, resulting in the recurrence (19). Thus, it remains critical to research molecular targets associated with lung cancer progression or chemoresistance, to develop novel therapeutic strategies for cancer treatment. Taken together, the results of the present study demonstrated that EZH2 silencing may sensitize lung cancer cells to the chemotherapeutic agent, CDDP. Thus, EZH2 may act as a novel target of lung cancer progression.

EZH2 has been demonstrated to act as a transcriptional inhibitor and is a polycomb group protein (20). Previous studies have reported that EZH2 is overexpressed in several types of cancer (21,22). For example, EZH2 promotes viability and migration of breast cancer cells (23). The present study screened the GEO database using the key words 'lung cancer', 'Homo sapiens' and 'Expression profiling by array or sequencing', identifying the GSE19804 dataset with sufficient samples for data analysis, including 60 adjacent non-tumor and 60 tumor samples. Both bioinformatics and western blot analyses demonstrated that the expression level of EZH2 was increased in lung carcinoma tissues and cell lines, which could promote carcinogenesis in lung cancer. Furthermore, survival analysis indicated that increased levels of EZH2 in lung carcinoma was associated with poor prognosis, suggesting that higher levels of EZH2 may be used as a latent molecular biomarker for the prognosis of cancer. After a large number of clinical observations and data statistics (24,25), it was revealed that the recurrence and metastasis of most tumor patients (80%) occurred ~3 years after radical surgery, while those of 10% of patients occurred ~5 years after treatment. Therefore, the present study analyzed the 3- and 5-year survival rates of patients with high EZH2 expression and low EZH2 expression. Similar results have also been demonstrated in other types of human malignant cancer, including colon (26), breast (27), lung (28), bladder (29), ovarian (30) and prostate cancer (31). Taken together, the results of the present study highlight a novel potential role of EZH2 as a molecular target for drug development in lung cancer.

Wang *et al* (32) reported that siRNA-mediated suppression of EZH2 in bladder cancer induces apoptosis; however, Rao *et al* (33) demonstrated that siRNA-EZH2 has no effect on apoptosis in ovarian cancer. The results of the present study are consistent with the findings by Wee *et al* (34), suggesting that the function of EZH2 varies in different types of cancer. Furthermore, EZH2 knockdown in A549 cells suppressed viability, whilst inducing apoptosis and producing cell cycle arrest in the G_1 phase. Taken together, these results confirm that EZH2 was associated with both tumor cell viability and apoptosis in lung cancer.

Metastasis is a complex process and can cause difficulties in the treatment of lung cancer (35), which has been defined as a multi-step process by which cell invasion contributes to metastasis (36). Previous studies have demonstrated that high expression levels of EZH2 was associated with cancer recurrence (37), distant metastasis (38), invasion (39) and angiogenesis (40) in numerous types of cancer, including melanoma and breast cancer. EZH2 is an adhesion protein expressed in breast and gastric cancer that promotes cancer metastasis by promoting ribosome synthesis; ribosomes are the cellular components that produce proteins, and their increased synthesis provides the conditions for cell metastasis (41). The results of the present study indicated that transfection with siRNA-EZH2 in lung cancer cells significantly inhibited invasion and migration. Furthermore, the expression levels of the EMT pathway proteins verified the molecular mechanisms of metastasis. Thus, EZH2 is a protein involved in the migration and invasion of lung cancer cells, whereby increased EZH2 expression may have a selective advantage on the migratory and invasive abilities of lung cancer cells. The detection of EZH2 expression can be performed as an additional tool to identify patients with lung cancer, with tumor progression and metastatic risk.

EPZ-6438 is a novel EZH2-specific inhibitor, which has demonstrated efficacy in different types of cancer, such as non-Hodgkin's lymphoma (42,43). In the present study, EPZ-6438 was used in combination with CDDP, which was demonstrated to have an additive effect on lung cancer cells. Treatment with the EZH2 inhibitor enhanced the CDDP-induced inhibition of cell viability and promoted apoptosis. However, further investigations into the molecular

mechanism underlying EZH2 in the response of CDDP are required. Notably, the results of the present study highlight the potential applications of EZH2 inhibitors in future clinical treatment interventions and anti-chemotherapy resistance. Further studies should perform additional downstream experiments to reveal the underlying molecular mechanism and should verify the present results using animal models, which are the limitations of the present study.

In conclusion, the results of the present study demonstrated that EZH2 played a vital role in molecular diagnosis and in the CDDP response of lung cancer. Suppression of EZH2 inhibited tumorigenesis and enhanced chemosensitivity, thus suggesting that EZH2 may be used as a novel molecular therapeutic target for lung carcinoma.

Acknowledgements

Not applicable.

Funding

The present study was funded by the Shanghai Sailing Program (grant no. 17YF1415800) and the National Natural Science Foundation of China (grant no. 81802803).

Availability of data and materials

All data generated or analyzed during this study are included in this published article. The datasets generated and/or analyzed during the current study (GSE19804 and GSE30219) are available in the GEO repository (https://www.ncbi.nlm.nih.gov/geo/).

Authors' contributions

ZC, WW and ZD designed the study and analyzed the data. WW, HW, WZ and YH performed the experiments. ZC drafted the initial manuscript. All authors read and approved the final manuscript.

Ethics approval and consent to participate

Not applicable.

Patient consent for publication

Not applicable.

Competing interests

The authors declare that they have no competing interests.

References

1. Pietrzak S, Wójcik J, Scott RJ, Kashyap A, Grodzki T, Baszuk P, Bielewicz M, Marciniak W, Wójcik N, Dębniak T, *et al*: Influence of the selenium level on overall survival in lung cancer. J Trace Elem Med Biol 56: 46-51, 2019.
2. Zhang L, Pu D, Liu D, Wang Y, Luo W, Tang H, Huang Y and Li W: Identification and validation of novel circulating biomarkers for early diagnosis of lung cancer. Lung Cancer 135: 130-137, 2019.
3. Peng A, Li G, Xiong M, Xie S and Wang C: Role of surgery in patients with early stage small-cell lung cancer. Cancer Manag Res 11: 7089-7101, 2019.
4. Nix MG, Rowbottom CG, Vivekanandan S, Hawkins MA and Fenwick JD: Chemoradiotherapy of locally-advanced non-small cell lung cancer: Analysis of radiation dose-response, chemotherapy and survival-limiting toxicity effects indicates a low α/β ratio. Radiother Oncol 143: 58-65, 2020.
5. Naghizadeh S, Mohammadi A, Baradaran B and Mansoori B: Overcoming multiple drug resistance in lung cancer using siRNA targeted therapy. Gene 714: 143972, 2019.
6. Wang X, Hua Y, Xu G, Deng S, Yang D and Gao X: Targeting EZH2 for glioma therapy with a novel nanoparticle-siRNA complex. Int J Nanomedicine 14: 2637-2653, 2019.
7. Sellers WR and Loda M: The EZH2 polycomb transcriptional repressor-a marker or mover of metastatic prostate cancer? Cancer Cell 2: 349-350, 2002.
8. Xu J, Wang Z, Lu W, Jiang H, Lu J, Qiu J and Ye G: EZH2 promotes gastric cancer cells proliferation by repressing p21 expression. Pathol Res Pract 215: 152374, 2019.
9. Chien YC, Liu LC, Ye HY, Wu JY and Yu YL: EZH2 promotes migration and invasion of triple-negative breast cancer cells via regulating TIMP2-MMP-2/-9 pathway. Am J Cancer Res 8: 422-434, 2018.
10. Guo S, Li X, Rohr J, Wang Y, Ma S, Chen P and Wang Z: EZH2 overexpression in different immunophenotypes of breast carcinoma and association with clinicopathologic features. Diagn Pathol 11: 41, 2016.
11. Han L, Zhang HC, Li L, Li CX, Di X and Qu X: Downregulation of long noncoding RNA HOTAIR and EZH2 induces apoptosis and inhibits proliferation, invasion, and migration of human breast cancer cells. Cancer Biother Radiopharm 33: 241-251, 2018.
12. Mu Z, Li H, Fernandez SV, Alpaugh KR, Zhang R and Cristofanilli M: EZH2 knockdown suppresses the growth and invasion of human inflammatory breast cancer cells. J Exp Clin Cancer Res 32: 70, 2013.
13. Lu TP, Tsai MH, Lee JM, Hsu CP, Chen PC, Lin CW, Shih JY, Yang PC, Hsiao CK, Lai LC and Chuang EY: Identification of a novel biomarker, SEMA5A, for non-small cell lung carcinoma in nonsmoking women. Cancer Epidemiol Biomarkers Prev 19: 2590-2597, 2010.
14. Dong S, Men W, Yang S and Xu S: Identification of lung adenocarcinoma biomarkers based on bioinformatic analysis and human samples. Oncol Rep 43: 1437-1450, 2020.
15. Rousseaux S, Debernardi A, Jacquiau B, Vitte AL, Vesin A, Nagy-Mignotte H, Moro-Sibilot D, Brichon PY, Lantuejoul S, Hainaut P, *et al*: Ectopic activation of germline and placental genes identifies aggressive metastasis-prone lung cancers. Sci Transl Med 5: 186ra66, 2013.
16. Singh C and Roy-Chowdhuri S: Quantitative real-time PCR: Recent advances. Methods Mol Biol 1392: 161-176, 2016.
17. Kramer N, Walzl A, Unger C, Rosner M, Krupitza G, Hengstschläger M and Dolznig H: In vitro cell migration and invasion assays. Mutat Res 752: 10-24, 2013.
18. Khorrami M, Jain P, Bera K, Alilou M, Thawani R, Patil P, Ahmad U, Murthy S, Stephans K, Fu P, *et al*: Predicting pathologic response to neoadjuvant chemoradiation in resectable stage III non-small cell lung cancer patients using computed tomography radiomic features. Lung Cancer 135: 1-9, 2019.
19. Isla D, De Las Peñas R, Insa A, Marsé R, Martínez-Banaclocha N, Mut P, Morán T, Sala MA, Massuti B, Ortega AL, *et al*: Oral vinorelbine versus etoposide with cisplatin and chemo-radiation as treatment in patients with stage III non-small cell lung cancer: A randomized phase II (RENO study). Lung Cancer 135: 161-168, 2019.
20. Ang PP, Tan GC, Karim N and Wong YP: Diagnostic value of the EZH2 immunomarker in malignant effusion cytology. Acta Cytol 64: 248-255, 2020.
21. Drelon C, Berthon A, Mathieu M, Ragazzon B, Kuick R, Tabbal H, Septier A, Rodriguez S, Batisse-Lignier M, Sahut-Barnola I, *et al*: EZH2 is overexpressed in adrenocortical carcinoma and is associated with disease progression. Hum Mol Genet 25: 2789-2800, 2016.
22. Herviou L, Jourdan M, Martinez AM, Cavalli G and Moreaux J: EZH2 is overexpressed in transitional preplasmablasts and is involved in human plasma cell differentiation. Leukemia 33: 2047-2060, 2019.
23. Puppe J, Opdam M, Schouten PC, Jóźwiak K, Lips E, Severson T, van de Ven M, Brambillasca C, Bouwman P, van Tellingen O, *et al*: EZH2 Is overexpressed in BRCA1-like breast tumors and predictive for sensitivity to high-dose platinum-based chemotherapy. Clin Cancer Res 25: 4351-4362, 2019.

24. Yan X, Jiao SC, Zhang GQ, Guan Y and Wang JL: Tumor-associated immune factors are associated with recurrence and metastasis in non-small cell lung cancer. Cancer Gene Ther 24: 57-63, 2017.
25. Fang D, Zhang D and Zhang R: Study of recurrence and metastasis after radical resection of carcinoma of the lung. Zhonghua Zhong Liu Za Zhi 21: 284-286, 1999 (In Chinese).
26. Katona BW, Liu Y, Ma A, Jin J and Hua X: EZH2 inhibition enhances the efficacy of an EGFR inhibitor in suppressing colon cancer cells. Cancer Biol Ther 15: 1677-1687, 2014.
27. Pourakbar S, Pluard TJ, Accurso AD and Farassati F: Ezh2, a novel target in detection and therapy of breast cancer. Onco Targets Ther 10: 2685-2687, 2017.
28. Geng J, Li X, Zhou Z, Wu CL, Dai M and Bai X: EZH2 promotes tumor progression via regulating VEGF-A/AKT signaling in non-small cell lung cancer. Cancer Lett 359: 275-287, 2015.
29. Martínez-Fernández M, Rubio C, Segovia C, López-Calderón FF, Dueñas M and Paramio JM: EZH2 in bladder cancer, a promising therapeutic target. Int J Mol Sci 16: 27107-27132, 2015.
30. Yi X, Guo J, Guo J, Sun S, Yang P, Wang J, Li Y, Xie L, Cai J and Wang Z: EZH2-mediated epigenetic silencing of TIMP2 promotes ovarian cancer migration and invasion. Sci Re 7: 3568, 2017.
31. Chinaranagari S, Sharma P and Chaudhary J: EZH2 dependent H3K27me3 is involved in epigenetic silencing of ID4 in prostate cancer. Oncotarget 5: 7172-7182, 2014.
32. Wang Y, Xiang W, Wang M, Huang T, Xiao X, Wang L, Tao D, Dong L, Zeng F and Jiang G: Methyl jasmonate sensitizes human bladder cancer cells to gambogic acid-induced apoptosis through down-regulation of EZH2 expression by miR-101. Br J Pharmacol 171: 618-635, 2014.
33. Rao ZY, Cai MY, Yang GF, He LR, Mai SJ, Hua WF, Liao YJ, Deng HX, Chen YC, Guan XY, *et al*: EZH2 supports ovarian carcinoma cell invasion and/or metastasis via regulation of TGF-beta1 and is a predictor of outcome in ovarian carcinoma patients. Carcinogenesis 31: 1576-1583, 2010.
34. Wee ZN, Li Z, Lee PL, Lee ST, Lim YP and Yu Q: EZH2-mediated inactivation of IFN-γ-JAK-STAT1 signaling is an effective therapeutic target in MYC-driven prostate cancer. Cell Rep 8: 204-216, 2014.
35. Dar WR and Mir MH: Pontine metastasis as an initial presentation of lung cancer. Neurol India 67: 918-920, 2019.
36. Aminorroaya A, Khoshniatnikoo M, Farrokhpour H, Vafaeimanesh J and Bagherzadeh M: Squamous cell carcinoma of the lung and pulmonary metastasis of papillary thyroid carcinoma: A case report. J Med Case Rep 13: 259, 2019.
37. Nakagawa S, Okabe H, Ouchi M, Tokunaga R, Umezaki N, Higashi T, Kaida T, Arima K, Kitano Y, Kuroki H, *et al*: Enhancer of zeste homolog 2 (EZH2) regulates tumor angiogenesis and predicts recurrence and prognosis of intrahepatic cholangiocarcinoma. HPB (Oxford) 20: 939-948, 2018.
38. Alford SH, Toy K, Merajver SD and Kleer CG: Increased risk for distant metastasis in patients with familial early-stage breast cancer and high EZH2 expression. Breast Cancer Res Treat 132: 429-437, 2012.
39. Manning CS, Hooper S and Sahai EA: Intravital imaging of SRF and notch signalling identifies a key role for EZH2 in invasive melanoma cells. Oncogene 34: 4320-4332, 2015.
40. Crea F, Fornaro L, Bocci G, Sun L, Farrar WL, Falcone A and Danesi R: EZH2 inhibition: Targeting the crossroad of tumor invasion and angiogenesis. Cancer Metastasis Rev 31: 753-761, 2012.
41. Xu Z, Sun Y, Guo Y, Qin G, Mu S, Fan R, Wang B, Gao W, Wu H, Wang G and Zhang Z: NF-YA promotes invasion and angiogenesis by upregulating EZH2-STAT3 signaling in human melanoma cells. Oncol Rep 35: 3630-3638, 2016.
42. Chen J, Chen X, Yao J, Li M and Yang X: The combination of decitabine and EPZ-6438 effectively facilitate adipogenic differentiation of induced pluripotent stem cell-derived mesenchymal stem cells. Biochem Biophys Res Commun 516: 307-312, 2019.
43. Knutson SK, Kawano S, Minoshima Y, Warholic NM, Huang KC, Xiao Y, Kadowaki T, Uesugi M, Kuznetsov G, Kumar N, *et al*: Selective inhibition of EZH2 by EPZ-6438 leads to potent antitumor activity in EZH2-mutant non-Hodgkin lymphoma. Mol Cancer Ther 13: 842-854, 2014.